JACC: BASIC TO TRANSLATIONAL SCIENCE VOL. ■, NO. ■, 2023



PRECLINICAL RESEARCH

# Neuregulin-1β Improves Uremic Cardiomyopathy and Renal Dysfunction in Rats

Márta Sárközy, MD, PhD,[a,b] Simon Watzinger, MSc,[c] Zsuzsanna Z.A. Kovács, MD, PhD,[a,b] Eylem Acar, BSc,[c] Fanni Márványkövi, MD,[a,b] Gergő Szűcs, MD, PhD,[a,b] Gülsüm Yilmaz Lauber, BSc,[c] Zsolt Galla, PharmD, PhD,[d] Andrea Siska, MSc,[e] Imre Földesi, PharmD, PhD,[e] Attila Fintha, MD, PhD,[f] András Kriston, MSc,[g,h,i] Ferenc Kovács, MSc,[g,h,i] Péter Horváth, MSc, PhD,[g,h,i] Bence Kővári, MD, PhD,[j] Gábor Cserni, MD, PhD, DSc,[j] Tibor Krenács, MSc, PhD, DSc,[f] Petra Lujza Szabó, MSc, PhD,[c] Gábor Tamás Szabó, MD, PhD,[c] Péter Monostori, PharmD, PhD,[d] Karin Zins, MD, PhD,[k] Dietmar Abraham, MD, PhD, DSc,[k] Tamás Csont, MD, PhD,[a,b] Peter Pokreisz, MSc, PhD,[c] Bruno K. Podesser, MD, PhD, DSc,[c] Attila Kiss, MSc, PhD[c]

## VISUAL ABSTRACT

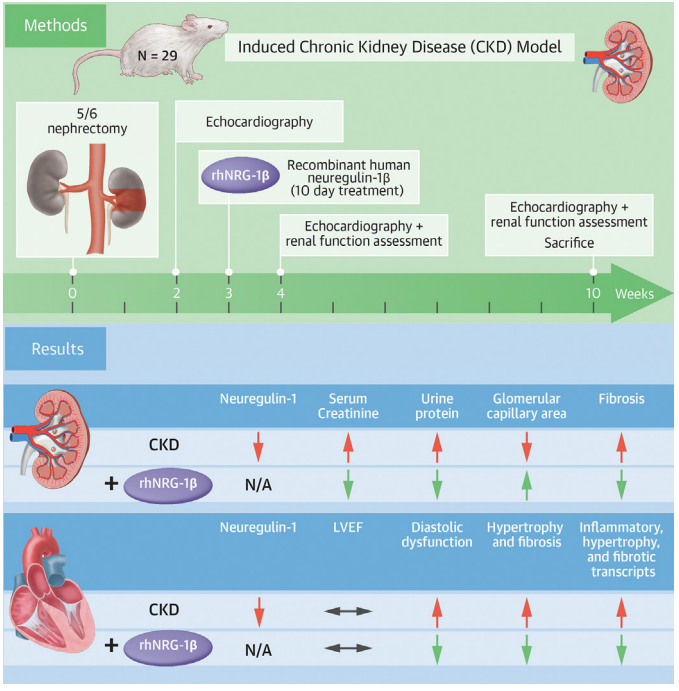


Sárközy M, et al. J Am Coll Cardiol Basic Trans Science. 2023;■(■):■-■.

## HIGHLIGHTS

- **Uremic cardiomyopathy is characterized by LVH, diastolic dysfunction, and cardiac fibrosis, leading to HF.**
- **Dysregulation of NRG-1β signaling is a known contributor to HF.**
- **rhNRG-1β alleviated the progression of uremic cardiomyopathy and kidney dysfunction.**
- **RhNRG-1β is a novel promising candidate in the prevention and therapy of uremic cardiomyopathy and renal dysfunction.**
- **Further studies are needed to translate the beneficial effects of rhNRG-1β in patients with CKD.**

From the [a]MEDICS Research Group, Department of Biochemistry, Albert Szent-Györgyi Medical School, University of Szeged, Szeged, Hungary; [b]Interdisciplinary Center of Excellence, University of Szeged, Szeged, Hungary; [c]Ludwig Boltzmann Institute for Cardiovascular Research at Center for Biomedical Research and Translational Surgery, Medical University of Vienna, Vienna, Austria; [d]Metabolic and Newborn Screening Laboratory, Department of Pediatrics, Albert Szent-Györgyi Medical School, University

ISSN 2452-302X https://doi.org/10.1016/j.jacbts.2023.03.003

## ABBREVIATIONS AND ACRONYMS

**ACE1** = angiotensin-converting enzyme-1

**Ang II** = angiotensin II

**CKD** = chronic kidney disease

**CVD** = cardiovascular disease

**ELISA** = enzyme-linked immunosorbent assay

**HE** = hematoxylin and eosin*

**HF** = heart failure

**LV** = left ventricular

**LVEDD** = left ventricular end-diastolic diameter

**LVEDV** = left ventricular end-diastolic volume

**LVH** = left ventricular hypertrophy

**NRG** = neuregulin

***nox2*** = NADPH-oxidase isoform 2

***nox4*** = NADPH-oxidase isoform 4

***Nppb*** = B-type natriuretic peptide

**PSFG** = picrosirius red/fast green*

**rhNRG** = human recombinant neuregulin

**RT-qPCR** = real-time quantitative polymerase chain reaction

**TGF** = transforming growth factor

**TRIS** = tris(hydroxymethyl) aminomethane hydrochloride

## SUMMARY

Chronic kidney disease is a global health problem affecting 10% to 12% of the population. Uremic cardiomyopathy is often characterized by left ventricular hypertrophy, fibrosis, and diastolic dysfunction. Dysregulation of neuregulin-1β signaling in the heart is a known contributor to heart failure. The systemically administered recombinant human neuregulin-1β for 10 days in our 5/6 nephrectomy–induced model of chronic kidney disease alleviated the progression of uremic cardiomyopathy and kidney dysfunction in type 4 cardiorenal syndrome. The currently presented positive preclinical data warrant clinical studies to confirm the beneficial effects of recombinant human neuregulin-1β in patients with chronic kidney disease. (J Am Coll Cardiol Basic Trans Science 2023;■:■–■) 

Chronic kidney disease (CKD) is a public health problem affecting 1 out of 10 people owing to the growing prevalence of its primary causes, including aging, diabetes mellitus, hypertension, and hyperlipidemia.[1,2] CKD and end-stage renal disease patients have a 5 to 10 times increased risk of developing cardiovascular diseases (CVDs) than the age-matched population without CKD.[3,4] CKD-associated chronic and often irreversible structural and functional changes of the heart are called uremic cardiomyopathy (ie, type 4 cardiorenal syndrome).[5-7] It is characterized by left ventricular hypertrophy (LVH), diastolic dysfunction, capillary rarefaction, endothelial dysfunction, and cardiac fibrosis, ultimately leading to heart failure (HF).[7,8]

In general, kidney function is often impaired in patients with HF with preserved ejection fraction and patients with HF with reduced ejection fraction; conversely, chronic HF aggravates renal dysfunction in cardiorenal syndromes.[5] Dysfunction of each organ can induce and perpetuate injury in the other via complex hemodynamic, neurohormonal, and biochemical pathways.[5-7] Multiple factors and mechanisms may contribute to the development of uremic cardiomyopathy and type 4 cardiorenal syndrome. These factors include non-CKD-specific mechanisms (ie, shared in CVDs and CKD) such as pressure and volume overload with overactivation of the renin-angiotensin-aldosterone system and sympathetic nervous system, hypertension, endothelial injury, inflammation, and increased nitro-oxidative stress, and CKD-specific factors such as circulating uremic toxins (eg, indoxyl-sulfate and p-cresyl sulfate) and renal anemia.[7,8] The protein-bound and consequently nondialyzable uremic toxins produced by colonic microbes are probably the most critical factors in the development of LVH and fibrosis in patients with CKD.[9,10] Indeed, the disproportionally high incidence of cardiovascular events and the severity of LVH were decreased dramatically after successful kidney transplantations.[10]

However, the precise molecular mechanisms in the development of uremic cardiomyopathy remain unclear. Despite the broad availability of standard medications to control the underlying diseases, including hypertension, diabetes mellitus, and hyperlipidemia, the high cardiovascular morbidity and mortality among patients with CKD remain unresolved.[8] Therefore, novel multitarget agents able to alleviate the severity of uremic cardiomyopathy are urgently needed.

Growing evidence demonstrates that dysregulation of neuregulin-1 (NRG-1β) signaling via its receptors

of Szeged, Hungary; [e]Department of Laboratory Medicine, Albert Szent-Györgyi Medical School, University of Szeged, Szeged, Hungary; [f]Department of Pathology and Experimental Cancer Research, Semmelweis University, Budapest, Hungary; [g]Synthetic and Systems Biology Unit, Biological Research Centre, Eötvös Loránd Research Network, Szeged, Hungary; [h]Single-Cell Technologies Ltd, Szeged, Hungary; [i]Institute for Molecular Medicine Finland (FIMM), University of Helsinki, Helsinki, Finland; [j]Department of Pathology, Albert Szent-Györgyi Medical School, University of Szeged, Szeged, Hungary; and the [k]Center for Anatomy and Cell Biology, Medical University of Vienna, Vienna, Austria.

The authors attest they are in compliance with human studies committees and animal welfare regulations of the authors' institutions and Food and Drug Administration guidelines, including patient consent where appropriate. For more information, visit the Author Center.

Manuscript received January 24, 2023; revised manuscript received March 1, 2023, accepted March 1, 2023.

ErbB (2, 3, and 4) could facilitate adverse cardiac remodeling and HF. NRG-1β is a stress-mediated paracrine transmembrane growth factor derived from endothelial cells.[11] It plays an essential role in embryonic cardiac development.[12] The dysregulation of NRG-1β expression is also linked to various CVDs such as myocardial infarction and HF.[12,13] Recombinant human NRG-1β (rhNRG-1β) protein administration has been reported to protect against myocardial ischemia/reperfusion injury and cardiac fibrosis and to stimulate cardiac repair in post-myocardial infarction remodeling.[11,13,14] Notably, Hopf et al[14] demonstrated that chronic administration of rhNRG-1β improved diabetes-induced passive stiffness in cardiomyocytes (CMs). A recent study demonstrated that the NRG-1β/ErbB signaling activation reduced myocardial macrophage infiltration, cytokine expression, and concomitant fibrosis in mice.[15] Indeed, macrophages and T cells could play a causal role in CM hypertrophy and diastolic dysfunction in uremic cardiomyopathy, but the significance of NRG-1β in CKD and uremic cardiomyopathy remains unknown.[16,17] Therefore, in our current study, we measured the cardiac and renal levels of NRG-1β and evaluated the effects of rhNRG-1β-therapy applied in a rat model of CKD.

## METHODS

**ETHICS APPROVAL.** This investigation conformed to the EU Directive 2010/63/EU and was approved by the regional Animal Research Ethics Committee of Csongrád County (XV.2598/2020, date of approval: 18 September 2020) and the University of Szeged in Hungary. All institutional and national guidelines for the care and use of laboratory animals were followed.

**ANIMALS.** In this study, a total of 29 adult male Wistar rats (*Rattus norvegicus*, 9-10 weeks old, 350-380 g) were housed in individually ventilated cages (Tecniplast Sealsafe IVC system) and were maintained with a 12 hour:12 hour light/dark cycles in a temperature-controlled room (22 ± 2 °C; relative humidity 55% ± 10%) throughout the study. Standard rat chow and tap water were supplied ad libitum.

**EXPERIMENTAL SETUP AND PROTOCOL.** Control animals underwent a sham operation (n = 9), and 20 animals received a subtotal 5/6 nephrectomy in 2 phases to induce CKD (Supplemental Figure 1), as described previously.[18,19] After the operations, rats were followed for 10 weeks. On the first day of the third follow-up week, rats were randomized into 3 treatment groups: 1) saline-treated (intravenous [IV] 0.5 mL/kg/d) sham-operated group; 2) saline-treated (IV 0.5 mL/kg/d) CKD group; and 3) and rhNRG-1β-treated (IV 10 μg/kg/d in 0.5 mL/kg end volume, Stemcell Technologies) CKD group. The animals were treated with saline or rhNRG-1β for 10 consecutive days via the tail veins, and the dosage and experimental protocol were selected based on previous studies.[13,20] During the follow-up time, 2 animals died in the rhNRG-1β-treated CKD group. At follow-up weeks 2, 4, and 10, cardiac morphology and function were assessed by transthoracic echocardiography (Supplemental Figure 1).[18,19] The animals were placed into metabolic cages (Tecniplast Metabolic Cage System) at weeks 4 and 10 for 24 hours to measure urine volume, creatinine, and protein levels (Supplemental Figure 1).[19,21] Blood was collected from the saphenous vein at week 4 and from the abdominal aorta at week 10 to measure serum carbamide (ie, urea), creatinine, and lipid levels as well as plasma uremic toxin levels at the endpoint.[19,21,22] At the termination of the experiment, body weight was measured, then rats were anesthetized with sodium pentobarbital (Euthasol; 40 mg/kg, intraperitoneally; Produlab Pharma b.v.), and an invasive blood pressure measurement was performed in the right femoral artery in a subgroup of animals (Supplemental Figure 1).[19] After the blood pressure measurement, the abdominal cavity was opened to collect 1.0 to 1.5 mL of blood from the aorta. Then sodium pentobarbital was overdosed (Euthasol, 200 mg/kg, intraperitoneally; Produlab Pharma b.v.) to euthanize the rats. Then the hearts, left kidneys, lungs, and tibias were isolated, and the blood was washed out in calcium-free Krebs-Henseleit solution. The hearts, kidneys, and lungs were weighed, left ventricles (LV) and right ventricles were separated and weighed, and the cross-section of the LV at the ring of the papillae and a middle cross-sectional ring of the left kidney were cut and fixed in 4% buffered formalin for histological analysis. Other parts of the LVs and kidneys were freshly frozen in liquid nitrogen and stored at −80 °C until further biochemical measurements. The development of CM hypertrophy, glomerular and tubular morphology, as well as cardiac and renal fibrosis in CKD, were verified on hematoxylin and eosin (HE) and picrosirius red/fast green (PSFG)-stained sections, respectively.[19,21] Additionally, inflammation in cardiac tissue and renal fibrosis were investigated by staining of CD68-positive macrophages and collagen-1 (COL1), respectively (see the detailed descriptions in the Supplemental Appendix). LV and renal NRG-1β protein levels were measured by enzyme-linked immunosorbent assay (ELISA). Markers associated with fibrosis, hypertrophy, inflammation, and nitro-oxidative stress were measured by real-time quantitative polymerase chain reaction (RT-qPCR) and

ELISA in LV tissue samples. In addition, expressions of ErbB2-4 isoforms in LV and renal samples were also measured by RT-qPCR. Cell culture experiments were performed in human ventricular cardiac fibroblasts (HVCF) and isolated adult mouse ventricular CMs isolated and cultured as previously described.[23-25]

**SUBTOTAL (5/6) NEPHRECTOMY MODEL.** Anesthesia was induced by intraperitoneal injection of pentobarbital sodium (Euthasol; 40 mg/kg; Produlab Pharma b.v.). At the first operation, 2 pieces of sutures (5-0 Mersilk; Ethicon) were placed around both poles of the left kidney, approximately at the one-third position. Then the sutures were gently ligated around the kidney. The one-third kidney on both ends was excised right beyond the ligatures. One week after the first operation, the animals were anesthetized again, and the right kidney was freed from the surrounding adipose tissue and the renal capsule, then pulled out of the incision gently. The adrenal gland was gently freed and placed back into the abdominal cavity. The renal blood vessels and the ureter were ligated, and the right kidney was removed. During sham operations, only the renal capsules were removed. After the surgeries, the incision was closed with continuous sutures, and povidone-iodine was applied to the surface of the skin. As a postoperative medication, subcutaneous 0.3 mg/kg nalbuphine hydrochloride (nalbuphine 10 mg/mL, Teva Pharmaceuticals Ltd) was administered for 4 days: twice on the first 2 days, then once on the third and fourth postoperative days. Enrofloxacin antibiotics (Enroxil 75 mg tablets, Krka; dissolved in tap water in 3.5 mg/L end concentration) were administered in the drinking water for 4 days after both surgeries.

**TRANSTHORACIC ECHOCARDIOGRAPHY.** Cardiac morphology and function were assessed by transthoracic echocardiography as described previously.[19,21] Rats were anesthetized with 2% isoflurane (Forane, AESICA). Then, the chest was shaved, and the animal was placed supine on a heating pad. Two-dimensional, M-mode, Doppler, and tissue Doppler echocardiographic examinations were performed by the criteria of the American Society of Echocardiography with a Vivid IQ ultrasound system (General Electric Medical Systems) using a phased array 5.0- to 11.0-MHz transducer (12S-RS probe, General Electric Medical Systems). Data from 3 consecutive heart cycles were analyzed (EchoPac Dimension v201 software, General Electric Medical Systems) by an experienced investigator in a blinded manner. The mean values of the 3 measurements were calculated and used for statistical evaluation. Systolic and diastolic wall thickness parameters were obtained from the parasternal short axis view at the level of the papillary muscles (anterior and inferior walls) and the long axis view at the level of the mitral valve (septal and posterior walls). The LV diameters were measured using M-mode echocardiography from long axis views between the endocardial borders. Fractional shortening was used as a measure of cardiac contractility (fractional shortening = (LV end-diastolic diameter [LVEDD] - LV end-systolic diameter [LVEDD])/LVEDD × 100). Functional parameters, including LV end-diastolic volume (LVEDV) and LV end-systolic volume, were calculated on 4-chamber view images delineating the endocardial borders in diastole and systole. The ejection fraction was calculated using the formula (LVEDV − LV end-systolic volume)/LVEDV × 100. Diastolic function was assessed using pulse-wave Doppler across the mitral valve from the apical 4-chamber view and tissue Doppler images at the lateral and septal mitral annulus. Early mitral flow (E), septal mitral annulus (E') velocities and their ratio (E/E') indicate diastolic function. Heart rate was calculated using pulse-wave Doppler images during the measurement of transvalvular flow velocity profiles according to the length of 3 consecutive heart cycles measured between the start points of the E waves.

**ARTERIAL BLOOD PRESSURE MEASUREMENT.** A PE50 polyethylene catheter (Cole-Parmer) was inserted into the left femoral artery under sodium-pentobarbital anesthesia (Euthasol; 40 mg/kg; Produlab Pharma b.v.) at week 10. Blood pressure measurements were performed between 09:00 and 14:00 hours using a SEN-02 pressure transducer (MDE Ltd.) connected to an EXP-HG-1 amplifier (MDE Ltd.) and WS-DA data acquisition system (MDE Ltd.). Data evaluation was made by S.P.E.L. Advanced Haemosys software (MDE Ltd.).[19]

**SERUM AND URINE METABOLITE CONCENTRATIONS.** Urea and creatinine levels in serum were quantified by kinetic UV spectrophotometric method using urease and glutamate dehydrogenase enzymes according to the Jaffe's method. The reagents and the platform analyzers were from Roche Diagnostics (Hoffmann-La Roche Ltd.).[18,22] Creatinine clearance, an indicator of renal function, was calculated according to the standard formula (urine creatinine concentration [μM] × urine volume for 24 hours [mL])/(serum creatinine concentration [μmol/L] × 24 × 60 minutes). At weeks 4 and 10, urine volume, urine creatinine, and serum creatinine concentration were measured.[18,22] Total serum cholesterol, high-density lipoprotein cholesterol, and triglyceride levels were measured by a

Roche Cobas 8000 analyzer system using enzymatic colorimetric assays from Roche (Hoffmann-La Roche Ltd). Low-density lipoprotein (LDL) cholesterol was calculated according to Friedewald's formula.[19]

**PLASMA UREMIC TOXIN LEVELS.** The levels of plasma uremic toxins were measured according to previously published methodologies using ultra-high performance liquid chromatography-tandem mass spectrometry.[26,27] Multiple reaction monitoring transition of indoxyl sulfate was 211.9/131.9 using -50 V as declustering potential and -25 V as collision energy, with a retention time of 11.48 minutes. Multiple reaction monitoring transition of p-cresyl sulfate was 186.9/107.0 using -50 V as declustering potential and -26 V as collision energy, with a retention time of 12.50 minutes.

**HE AND PSFG STAININGS.** Formalin-fixed paraffin-embedded subvalvular areas of the LVs and the middle cross-sectional rings of the left kidneys were cut into 5-μm sections and were stained with HE or PSFG, as described previously.[19,28,29] Histological slides were scanned with a Pannoramic Midi II scanner (3DHistech Ltd.). Digital slide processing was performed in SlideViewer version 2.6 (last accessed on January 3, 2023). On the digital HE images, CM diameters and cross-sectional areas were measured to verify the development of LVH at the cellular level.

The Biology Image Analysis Software (BIAS 1.0, Single-Cell Technologies Ltd.) was used to evaluate HE images.[19,28,29] Image preprocessing was followed by deep learning-based cytoplasm segmentation. User-selected objects were forwarded to the feature extraction module configurable to extract properties from the selected cell components. The transverse CM diameter at the nuclear level and cell perimeter were measured in 100 (consecutive) CMs selected based on longitudinal orientation and mononucleation from a single cut surface (digitalized histological slide) of the LV tissue blocks. The BIAS software also calculated CM cross-sectional areas of the same cells.

Renal cell nucleus quantification was performed on HE-stained slides by QuantCenter (version 2.3) NuclearQuant module (3DHistech Ltd.). Tubule dilatation was measured by QuantCenter (version 2.3) HistoQuant module (3DHistech Ltd.) on HE-stained slides. Kidney cortex areas were annotated manually, and the proportion of white area was measured, representing tubular lumen areas.

Cardiac fibrosis was assessed on PSFG slides with a program developed in-house, as described previously.[19,21] Briefly, this program determines the proportion of red pixels in LV sections using 2 simple color filters. For each red-green-blue (RGB) pixel, the program calculates the color of the pixel in the hue-saturation-luminance color space. The first filter is used for detecting red portions of the image. The second filter excludes any white (empty) or light gray (residual dirt on the slide) pixel from further processing using a simple RGB threshold. In this way, the program groups each pixel into 2 sets: pixels considered red, and pixels considered green but not red, white, or grey. Red pixels in the first set correspond with connective tissue and fibrosis. Green pixels in the second set correspond with cardiac muscle. Dividing the number of elements in the first set by the number of elements in both sets gives the proportion of the connective tissue compartment of the heart area examined.

Renal interstitial fibrosis was measured by QuantCenter (version 2.3) HistoQuant module (3DHistech Ltd.) on PSFG-stained slides. Kidney cortex areas were manually annotated, and the proportion of red areas (red filter 123-221, green filter 13-153, blue filter 33-166) was measured, representing interstitial fibrosis.

**ASSESSMENT OF NRG-1 LEVELS IN LV AND KIDNEY SAMPLES.** The protein levels of NRG-1β were assessed by ELISA (E-EL-R0790 Elabscience) in the LV and kidney tissue sample extracts according to the manufacturer's protocol.

**NITROTYROSINE ASSESSMENT.** An ELISA kit for 3-nitrotyrosine measurement was purchased from Bioassay Technology Laboratory (Cat. No: E0019Ra). LVs were homogenized with an ultrasonicator (UP100H) in phosphate-buffered saline (PBS, pH 7.4) and then centrifuged at 3000 rpm for 20 minutes at 4 °C. After quantifying the supernatants' protein concentrations using the BCA Protein Assay Kit (Pierce Thermo Fisher Scientific Inc), 3-nitrotyrosine was measured according to the manufacturer's instructions. Optical densities were determined at 450 nanometers and amounts of analytes standardized to protein concentrations (nmol/g) were reported.

**ANGIOTENSIN-CONVERTING ENZYME-1 ACTIVITY MEASUREMENTS.** Angiotensin-converting enzyme-1 (ACE1) activity in kidney tissue samples was measured as described previously.[30] Briefly, tissue samples were weighed, and a proportional amount of 100 mM tris(hydroxymethyl)aminomethane hydrochloride (TRIS) buffer (pH 7.0) was added and then homogenized. The tissue homogenates were centrifuged at 13,000 rpm for 5 minutes, and the protein concentration of the supernatant was determined by Pierce BCA Protein Assay Kit (Thermo Fisher Scientific) using TECAN (SparkControl Magellan V2.2) plate

reader. ACE1 activity was determined using an artificial substrate (Abz-FRK(Dnp)P-OH (Peptide 2.0) in a reaction mixture containing 6 μL of 1 mg/mL tissue homogenates in 35-fold dilution in 100 mmol/L TRIS buffer, 50 mmol/L NaCl, and 10 μmol/L ZnCl2 in 96-well plates (Greiner-Bio One) at 37 °C. The fluorescence intensity change was detected by TECAN (SparkControl Magellan V2.2) plate reader, $\lambda_{ex}$ was 340 nm, and $\lambda_{em}$ was 405 nanometers. The changes in fluorescence intensity were detected in kinetic loops at 1-minute intervals for at least 30 minutes, and the intensity values were plotted as a function of reaction time. The fluorescence intensity values were fitted by linear regression (GraphPad Software). Only the linear part of the data with a correlation coefficient of $r > 0.95$ were accepted. ACE1 activity was calculated by the following equation: activity $= (S/k) \times D/P$; where $S$ is the rate of the increase in fluorescence intensity (1/min), $k$ is the change of fluorescence intensity during the complete cleavage of 1 pmol Abz-FRK(Dnp)P-OH substrate, $D$ is the dilution of the sample, and $P$ is the protein concentration (in mg/mL). One unit (1 U) corresponds with 1 pmol substrate cleavage in 1 minute by 1 mg of protein.

**CELL CULTURE EXPERIMENTS.** HVCF (Lonza) were cultured in a fibroblast basal medium supplemented with 0.1% insulin, 0.1% fibroblast growth factor, 0.1% GA-1000, and 10% fetal bovine serum (all Lonza) as previously described.[24] Cultures were washed with HEPES buffered saline (Lonza) when indicated and split at a confluency level of 70%. Cells were serum starved for 24 hours, with subsequent treatment with one of the following: 1) without treatment (control); 2) 20 ng/mL transforming growth factor (TGF)-β) (Abcam); 3) rhNRG-1β (40 ng/mL); and 4) rhNRG-1β (40 ng/mL, Stemcell Technologies) + ErbB3 antibody (1 μg/mL, R&D Systems) for an additional 24 hours. Then, total RNA was extracted, and RT-qPCR was performed. In addition, HCVFs on coverslips were used for immunocytochemistry. Cells washed in PBS were fixed in 4% paraformaldehyde for 10 minutes. After removal of the fixative by rinsing in PBS, cells were permeabilized with Triton X-100 (0.5% v/v in PBS) for 3 minutes and washed twice in PBS-Tween (PBS-T, 0.1% v/v). Then, the fixation solution was removed with 3 rinses with PBS. Coverslips were blocked using 5% bovine serum albumin and incubated with primary antibody (α-smooth muscle actin, Novusbio, 10 μg/mL) in bovine serum albumin 1% for 1 hour. The first antibody was revealed by the Texas-red conjugated secondary antibody (horse anti-mouse IgG antibody [H+L], Texas Red, Thermo Fischer Scientific Inc) for 1 hour, and counterstained for detection of nuclei for 10 minutes with 4,6-diamidino-2-phenylindole (Sigma-Aldrich). Coverslips mounted on glass slides in Permafluor aqueous mounting fluid (Beckman Coulter) were observed under confocal imaging (LSM 700, Zeiss).

Adult mouse ventricular CMs were isolated according to a method developed by Ackers-Johnson et al.[25] C57BL/6H mice were anesthetized with a mixture of ketamine and xylazine, and the hearts were harvested. CMs isolation was performed by enzymatic dissociation using perfusion buffer, 37 °C prewarmed 40 mL enzyme solution (collagenase II 0.5 mg/mL (Worthington Biochemical Corporation), collagenase IV 0.5 mg/mL (Worthington Biochemical Corporation), and Protease XIV 0.05 mg/mL, Sigma-Aldrich). CM-containing solution was filtered through 100-μm filters and applied to a 50-mL centrifugation tube. Filters were washed through with 7 mL of sterile stop buffer. The filtered CM solution was divided equally into two 15-mL centrifugation tubes, and cells were allowed to settle for 20 minutes. The supernatant was aspirated, and every pellet was resuspended in 4 mL of buffer 1, followed by 10 minutes of incubation. This process was repeated for buffer 2 and buffer 3. After 10 minutes of settling in buffer 3, every pellet was resuspended in 1 mL of culture medium, and cells were counted in a hemocytometer. Cells were diluted to 20,000 cells per mL by applying an appropriate volume of plating medium. Cells were seeded in laminin-coated plates and incubated at 37 °C. After 1 hour, only viably CMs have been attached to the laminin surface. The plating medium was aspirated, and cells were washed with a culture medium to remove dead and nonattaching cells. Afterward, CMs were covered with a fresh culture medium and incubated for 24 hours before experimental treatment. CMs were exposed to treatment within 24 hours after isolation. CMs were then treated with different compounds for 24 hours: 1) 20 ng/mL TGF-β; 2) 200 nmol/L angiotensin-II (ANG-II, Merck); or 3) 200 nmol/L Ang-II + 40 ng/mL NRG-1β. mRNA expression of B-type natriuretic peptide (*Nppb*), A-type natriuretic peptide, tumor necrosis factor-alpha, and NADPH-oxidase isoforms 2 and 4 (*Nox2* and *Nox4*) were assessed by RT-qPCR.

**TRANSCRIPTION PROFILING BY RT-qPCR.** Total RNA was extracted from LV and kidney samples as well as isolated primary adult mouse CMs and HVCFs using the RNeasy Mini Kit (Qiagen) and quantified by NanoDrop spectrophotometer as described previously.[23] The cDNAs prepared using the QuantiTect reverse transcription kit (Qiagen) were analyzed in

technical duplicates in 20-μL reaction volumes. The initial denaturation step of 15 minutes at 95 °C was followed by 45 cycles of 15 seconds 95 °C, 30 seconds 50 °C, and 30 seconds 72 °C, using a Rotor-Gene Q thermocycler with the accompanying software (Qiagen) for cycle threshold value analysis. Relative gene expression was calculated by the $2^{-\Delta\Delta Ct}$ method. The primers are listed in Supplemental Table 1.

**STATISTICAL ANALYSES.** All analyses were performed with GraphPad Prism Software (version 9.4, GraphPad Software Inc). The data distribution was checked for normality by the Shapiro-Wilk test. One-way analysis of variance was used for comparisons among groups, which reduces to a *t*-test for only 2 groups. In cases of significant differences between the groups, the Holm-Sidak (in cases of serum and urine data, blood pressure, echocardiographic and histology data, and organ weights) or Tukey's correction (in cases of RT-qPCR, ELISA, and cell culture experiment data) was used as the post hoc test for multiple pairwise comparisons. Repeated measures 2-way analysis of variance was used to compare longitudinal data among groups across multiple follow-up time points, followed by the Holm-Sidak post hoc test. All values are presented as mean ± SEM, and a $P$ value of $<0.05$ was accepted as a statistically significant difference. The corresponding table or figure legends describe specific sample numbers and statistical tests used for comparisons.

## RESULTS

**NRG-1β EXPRESSION IS SIGNIFICANTLY DECREASED IN THE LV AND KIDNEY IN CKD.** At week 10, NRG-1β expression markedly declined in both LV and kidney tissues in CKD rats compared with the sham group (**Figures 1A and 1B**).

**RhNRG-1β TREATMENT PRESERVED THE RENAL FUNCTION AND DECREASED THE CIRCULATING UREMIC TOXIN LEVELS IN CKD.** Serum carbamide and creatinine concentrations were significantly increased in the CKD group at weeks 4 and 10, suggesting an impaired renal function from week 4 onward (Supplemental Figure 1, Supplemental Table 2, **Figures 1C and 1D**). Urine protein concentration showed a tendency to increase at week 4 and a significant increase at week 10 in the CKD group, indicating worsening glomerular function (**Figure 1E**, Supplemental Table 2). Creatinine clearance, the main clinical renal functional parameter, was significantly decreased in the CKD group compared with the sham-operated group at both follow-up time points, showing the development of renal dysfunction from week 4 (**Figure 1F**, Supplemental Table 2). In the sham-operated group, the creatinine clearance was significantly increased at the endpoint compared with the week 4 value, which could be attributed to the growth of the animals (Supplemental Table 2).

Notably, the serum creatinine level was markedly decreased by the rhNRG-1β treatment in CKD at weeks 4 and 10 (**Figure 1D**, Supplemental Table 2). There was no significant difference in the urine protein level between the sham-operated and rhNRG-1β-treated CKD groups (**Figure 1E**, Supplemental Table 2). At week 10, creatinine clearance showed an increasing tendency in response to rhNRG-1β treatment compared with the CKD group (**Figure 1F**, Supplemental Table 2). Importantly, serum creatinine and urine protein levels did not show significant worsening in response to rhNRG-1β at week 10 compared with the week 4 values, suggesting the renoprotective role of rhNRG-1β in CKD (Supplemental Table 2). At the endpoint, both p-cresyl sulfate and indoxyl sulfate plasma levels were significantly elevated in CKD compared with the sham-operated group (**Figures 1G and 1H**). In contrast, the rhNRG-1β treatment helped to significantly reduce uremic toxin levels in comparison with the CKD group (**Figures 1G and 1H**).

**RhNRG-1β REDUCED THE SERUM LDL CHOLESTEROL LEVEL IN CKD.** At weeks 4 and 10, the serum total cholesterol, high-density lipoprotein cholesterol, LDL cholesterol, and total cholesterol levels were significantly increased in the CKD group compared with the time-matched values of the sham-operated group (Supplemental Table 2). In response to the rhNRG-1β treatment, at week 4, the serum LDL level was not significantly different from the value of the sham-operated group, and at week 10, the serum LDL cholesterol level was significantly lower compared with the CKD group (Supplemental Table 2). Notably, serum total and high-density lipoprotein cholesterol levels showed a trend to decrease in response to rhNRG-1β to the time-matched values of the CKD group (Supplemental Table 2). At week 4, there was no significant difference in serum triglyceride levels between the groups (Supplemental Table 2). At week 10, serum triglyceride levels were significantly increased in the CKD group compared with the sham-operated group (Supplemental Table 2). There was no significant difference in the serum triglyceride levels between the sham-operated and rhNRG-1β-treated CKD groups at week 10 (Supplemental Table 2).

**RhNRG-1β TREATMENT DID NOT ALTER THE ELEVATED BLOOD PRESSURE IN CKD.** Systolic arterial blood pressure was significantly elevated in the CKD groups, independent of rhNRG-1β treatment as

**FIGURE 1 The Effects of rhNRG-1β on the Development of CKD at Week 10**

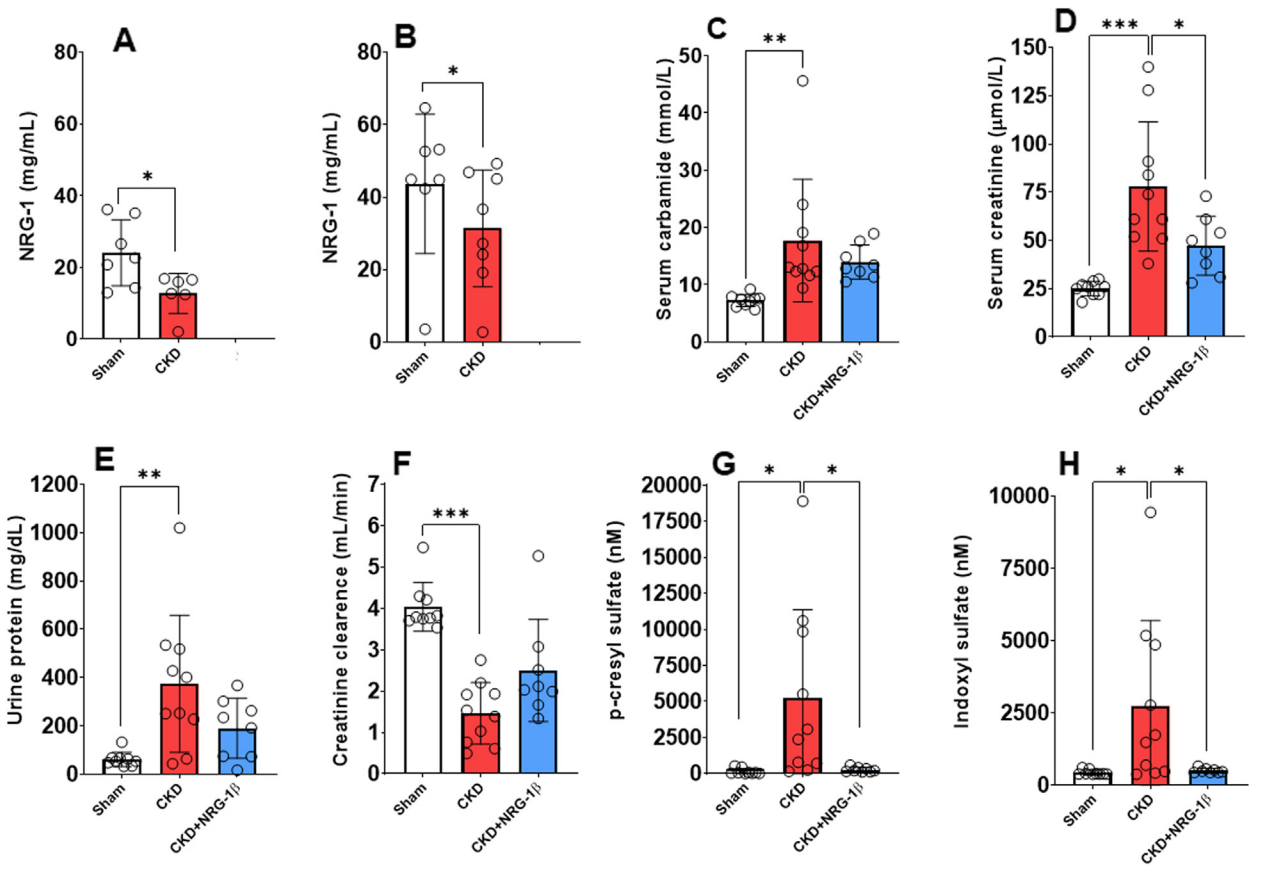


**(A)** NRG-1β protein expression in left ventricles and **(B)** kidney tissue at week 10 in 5/6 nephrectomized rats (unpaired Student *t* test). **(C)** Serum carbamide concentration, **(D)** serum creatinine concentration, **(E)** urine protein concentration, **(F)** creatinine clearance, **(G)** plasma p-cresyl sulfate concentration, and **(H)** plasma indoxyl sulfate concentration at week 10. Values are presented as mean ± SEM. *$P < 0.05$, **$P < 0.01$, ***$P < 0.001$, n = 7-10, 1-way analysis of variance, Holm-Sidak post hoc test. CKD = chronic kidney disease group; CKD + rhNRG-1β = recombinant human neuregulin-1β-treated chronic kidney disease group; LV = left ventricular; Sham = sham-operated group.

compared with the sham-operated group (CKD, 162 ± 7 mm Hg and CKD+rhNRG-1β, 163 ± 7 mm Hg vs sham-operated, 130 ± 9 mm Hg) at week 10. The diastolic blood pressure values showed a trend toward an increase in the CKD (112 ± 8 mm Hg; $P = 0.099$) and CKD+rhNRG-1β (113 ± 6 mm Hg; $P = 0.051$) groups compared with the sham-operated group (94 ± 6 mm Hg) at week 10. Similarly, the mean arterial blood pressure increased in the CKD (129 ± 8 mm Hg; $P = 0.058$) and CKD+rhNRG-1β groups (129 ± 7 mm Hg; $P = 0.047$, unpaired *t*-test) compared with the sham-operated (106 ± 7 mm Hg) group at week 10.

**RhNRG-1β LIMITED THE ECHOCARDIOGRAPHIC SIGNS OF LVH IN CKD.** There was no significant difference in the cardiac morphologic or functional parameters between the groups 2 and 4 weeks after the operations (Supplemental Tables 3 and 4, **Figures 2A to 2J**). At week 10, significantly increased wall thickness and markedly decreased LVEDD indicated the development of concentric LVH in the CKD group (Supplemental Table 4, **Figures 2A, 2G, and 2H**). The rhNRG-1β treatment decreased the LVH indices significantly and increased the LVEDD markedly compared with the values of the CKD group at week 10, pointing out its potential antihypertrophic effects (Supplemental Table 4, **Figures 2G and 2H**). In contrast, the rhNRG-1β-treated CKD group did not show any difference in the wall thicknesses (except for the diastolic septal wall) and LV diameters between weeks 4 and 10 values, indicating that rhNRG-1β treatment prevented the progression of LVH in our

**FIGURE 2** **The Effects of rhNRG-1β on Echocardiographic Parameters at Weeks 4 and 10**

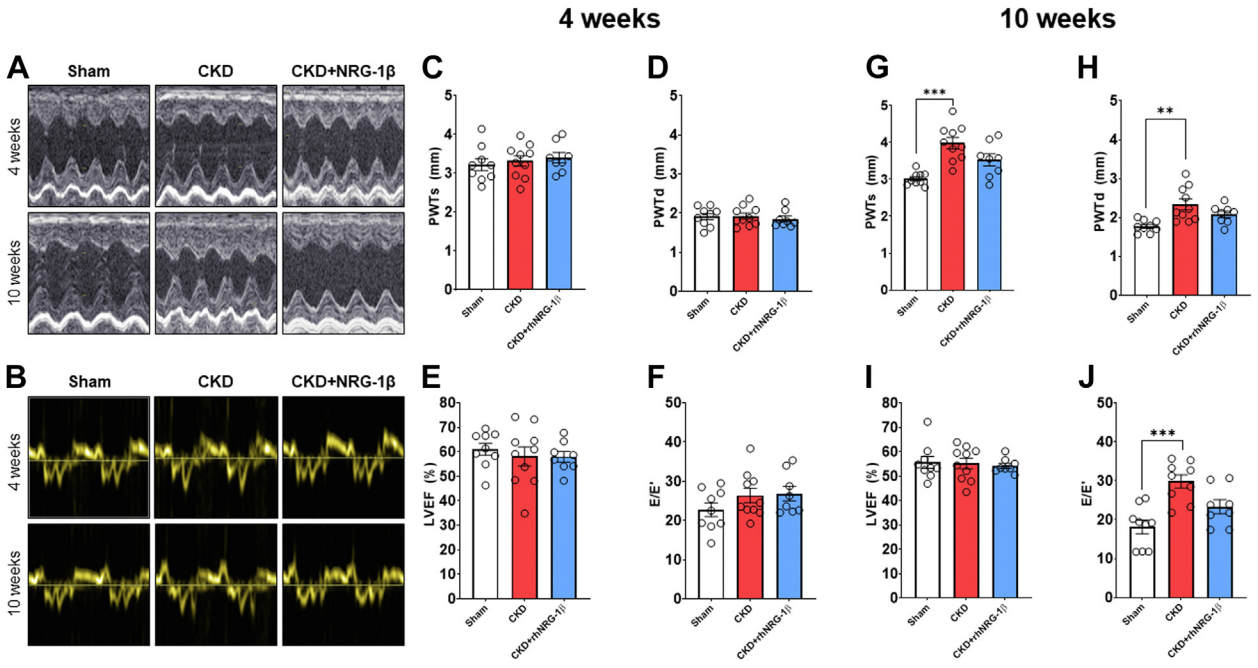


**(A)** Representative M-mode and **(B)** tissue Doppler images, **(C)** posterior wall thickness in systole (PWTs), and **(D)** diastole (PWTd), **(D)** left ventricular ejection fraction (EF), **(E)** ratio of early mitral flow velocity (E) and diastolic septal mitral annulus velocity (E') at week 4, **(F)** posterior wall thickness in systole (PWTs) and **(G)** diastole (PWTd) at week 10, **(H)** left ventricular EF, and **(I)** E/E' at week 10. Values are presented as mean ± SEM. * $P < 0.05$, ** $P < 0.01$, n = 7-10, one-way analysis of variance, Holm-Sidak post hoc test. Abbreviations as in Figure 1.

CKD model (Supplemental Table 4). In contrast, at week 10, anterior, posterior, and septal wall thicknesses increased further in the CKD group compared with the week 4 values, indicating the worsening LVH in CKD (Supplemental Table 4).

**RhNRG-1β AMELIORATED THE DIASTOLIC DYSFUNCTION IN CKD.** The global pump function represented by the ejection fraction was not significantly different among the groups at weeks 4 or 10, showing that the uremic cardiomyopathy persisted in the HF with preserved ejection fraction phase (Supplemental Table 4, **Figures 2E and 2I**). The mitral valve early flow velocity (E) was not significantly different between the groups, or the follow-up time points within the groups (Supplemental Table 4). At week 4, there **was** no significant difference in the septal mitral annulus velocity (E') or the E/E' ratio between the groups, probably owing to the lack of the development of severe LVH at this early time point of CKD (Supplemental Table 4, **Figure 2F**). In contrast, the E' was decreased significantly at week 10, and the E/E' was increased markedly in the CKD group compared with the sham-operated group indicating the progression of diastolic dysfunction in CKD (Supplemental Table 4, **Figure 2J**). At week 10, the E' velocity showed an increasing tendency in response to rhNRG-1β treatment compared with the CKD group (Supplemental Table 4). Moreover, in the rhNRG-1β-treated CKD group, there was no significant difference in the E' between the values at weeks 4 and 10 (Supplemental Table 4). Notably, there was no significant difference in the E/E' between the sham-operated and rhNRG-1β-treated CKD group at week 10, pointing out the beneficial lusitropic effect of rhNRG-1β on the diastolic function (Supplemental Table 4, **Figure 2J**).

**RhNRG-1β TREATMENT DECREASED THE MACROSCOPIC SIGNS OF LVH IN CKD.** The LV weight showed a significant increase in the CKD group compared with the sham-operated group indicating the macroscopic signs of LVH (Supplemental Table 5). In consonance with echocardiographic results, the rhNRG-1β treatment significantly reduced the LV weight compared with the CKD group (Supplemental Table 5). The remnant left kidney weight increased in the CKD and the rhNRG-1β-treated CKD group compared with the

**FIGURE 3 The Effects of rhNRG-1β on LV and Renal Morphology Assessed by Histology at Week 10**

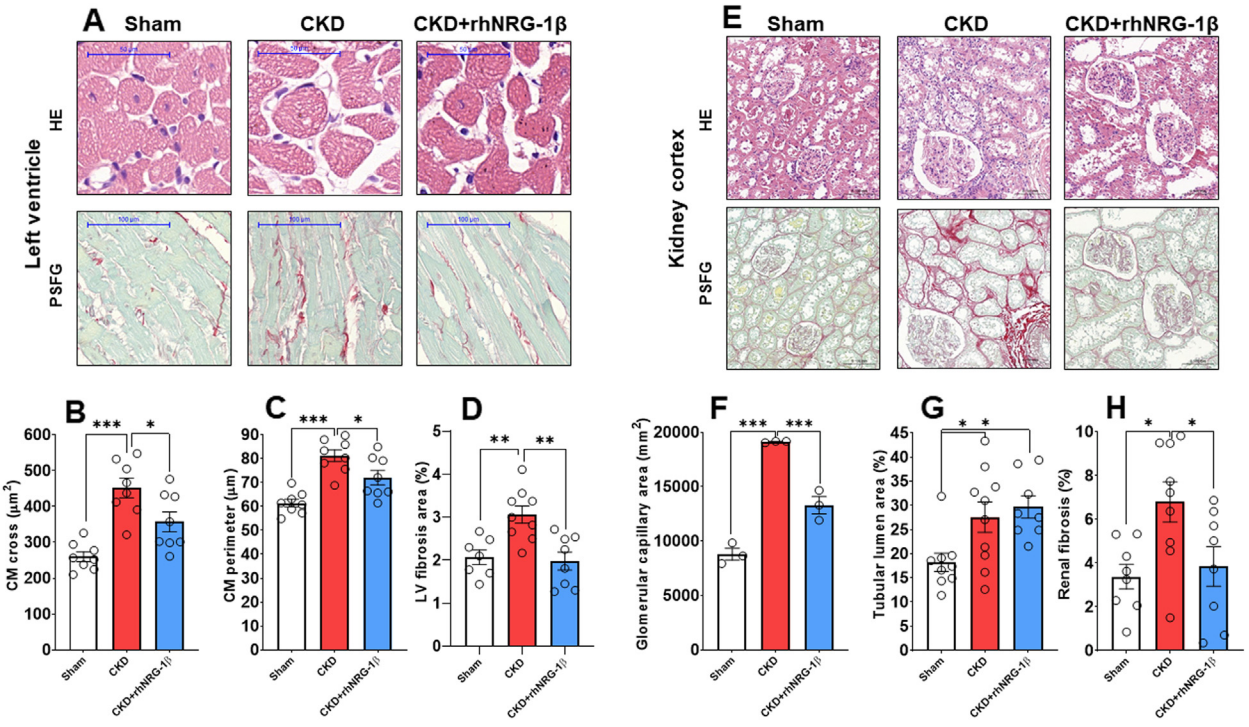


**(A)** Representative hematoxylin-eosin (HE)-stained slides and picrosirius red/fast green (PSFG)-stained slides of left ventricles. **(B)** cardiomyocyte cross-sectional areas, **(C)** perimeters, **(D)** left ventricular (LV) fibrosis, **(E)** representative HE-stained slides and PSFG-stained slides of the kidney tissue, **(F)** glomerular capillary area, **(G)** tubular lumen area, and **(H)** kidney interstitial fibrosis. In the case of left ventricles, scale bars represent 50 μm in the HE images and 100 μm in the PSFG images. In the case of kidney tissue, scale bars represent 100 μm in the HE images and 200 μm in the PSFG images. Values are presented as mean ± SEM, $*P < 0.05$, $**P < 0.01$, $***P < 0.001$, n = 7-10, one-way analysis of variance, Holm-Sidak post hoc test. Abbreviations as in Figure 1.

weight of the whole left kidney in the sham-operated group, suggesting compensatory renal hypertrophy in CKD (Supplemental Table 5).

**RhNRG-1β TREATMENT ALLEVIATED CM HYPERTROPHY AND LV INTERSTITIAL FIBROSIS.** CMs showed a significantly enlarged cross-sectional area and perimeter in the CKD group compared with the sham-operated group, confirming the development of LVH at the cellular level at week 10 (**Figures 3A to 3C**). The rhNRG-1β treatment significantly decreased the CM cross-sectional area and perimeter in CKD, validating the echocardiographic and macroscopic findings (**Figures 3A to 3C**). Significant interstitial fibrosis was found in the CKD group compared with the sham-operated group (**Figures 3A and 3D**), and this was markedly suppressed in the rhNRG-1β-treated group (**Figures 3A and 3D**).

**RhNRG-1β TREATMENT BETTER PRESERVED THE GLOMERULAR CAPILLARY AREA AND AMELIORATED KIDNEY INTERSTITIAL FIBROSIS.** The size of the glomeruli and their nuclear count were more prominent in the CKD groups compared with the sham-operated group, indicating the development of the compensatory enlargement of the remnant kidney (**Figures 3E and 3F**). Interestingly, the glomerular capillary areas were better preserved by the rhNRG-1β treatment in CKD (**Figures 3E and 3F**), whereas the tubular lumina dilation did not change proportionally by the administration of rhNRG-1β in CKD (**Figures 3E and 3G**). Marked interstitial fibrosis was found in the untreated CKD animals compared with the sham-operated group (**Figures 3E and 3H**, Supplemental Figure 2). The significant renal interstitial fibrosis was markedly ameliorated by the rhNRG-1β treatment in CKD (**Figures 3E and 3H**, Supplemental Figure 2).

**ACE1 ACTIVITY IN KIDNEY SAMPLES.** Compared with the sham-operated group, ACE1 activity was increased in CKD ($P = 0.065$) (Supplemental Figure 3), and a tendency toward declining ACE1

**FIGURE 4** The Effects of rhNRG-1β on mRNA Expressions in Uremic Cardiomyopathy in Left Ventricular Samples

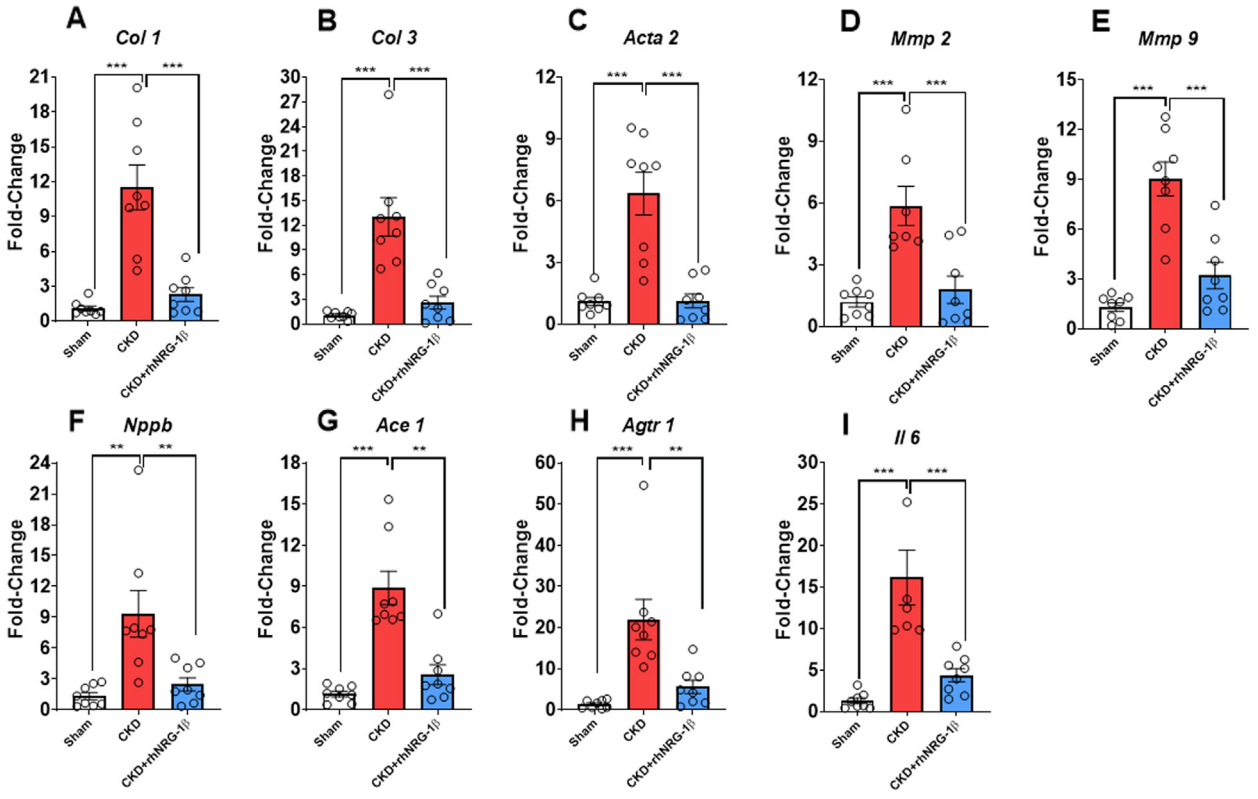


mRNA expressions of **(A)** *Col 1*, collagen 1; **(B)** *Col 3*, collagen 3; **(C)** alpha-smooth muscle actin (*Acta2*), alpha-smooth muscle actin; **(D)** *Mmp2*, matrix metalloprotease 2; **(E)** *Mmp9*, matrix metalloprotease 9; **(F)** *Nppb*, B-type natriuretic peptide; **(G)** *Ace1*, angiotensin-converting enzyme; **(H)** *Agtr1*, angiotensin II type 1 receptor; and **(I)** *Il6*, interleukin 6 in left ventricles. Data are expressed as mean ± SEM; n = 8/group, $^{**}P < 0.01$, $^{***}P < 0.001$, one-way analysis of variance, Tukey post hoc test. Abbreviations as in Figure 1.

activity (approximately 20%) was found in kidney tissue samples after the rhNRG-1β treatment in comparison to the untreated CKD group (Supplemental Figure 3).

**RhNRG-1β TREATMENT DECREASED THE OVEREXPRESSION OF CARDIAC INFLAMMATION, HYPERTROPHY, AND FIBROSIS MARKERS IN CKD.** Transcript levels of *Col1*, collagen-3 (*Col3*), alpha-smooth muscle actin, matrix metalloprotease-2, matrix metalloprotease-9, *Nppb*, angiotensin-converting enzyme 1 (*Ace1*), and angiotensin II (ang II) receptor type 1 (*Agtr1*) were significantly increased in the CKD group compared with the sham-operated group supporting our echocardiographic and histology findings (Figures 4A to 4H). Furthermore, CKD animals also displayed increased *Il6* mRNA expression (Figure 4I) and cardiac CD68-positive macrophage infiltration (Supplemental Figure 4). In contrast, these fibrotic, inflammatory, and hypertrophic markers were significantly blunted in response to the rhNRG-1β treatment (Figures 4A to 4I, Supplemental Figure 4).

To further validate the antifibrotic effect of NRG-1β, we investigated its effect on HVCFs exposed to TGF-β in vitro in the presence or absence of rhNRG-1β using alpha-smooth muscle actin immunofluorescent staining (Figure 5A). The overexpression of α-smooth muscle actin on TGF-β exposure was accompanied by elevated transcript levels of *Col1*, *Col3*, and the collagen cross-linking lysyl oxidase-1 (Figures 5B to 5E). These changes were ameliorated significantly in HVCFs co-treated with rhNRG-1β.

The expressions of ErbB 2, 3, and 4 mRNA levels were measured both in LV and kidney samples (Supplemental Figures 5A to 5E). *ErbB3* expression was significantly decreased in kidney samples and showed a tendency to preserve its expression by the administration of rhNRG-1β (Supplemental Figure 5B). The expression of *ErbB2* and *ErbB4* in

**FIGURE 5 The Effects of rhNRG-1β on mRNA Expressions in Human Ventricular Cardiac Fibroblasts**

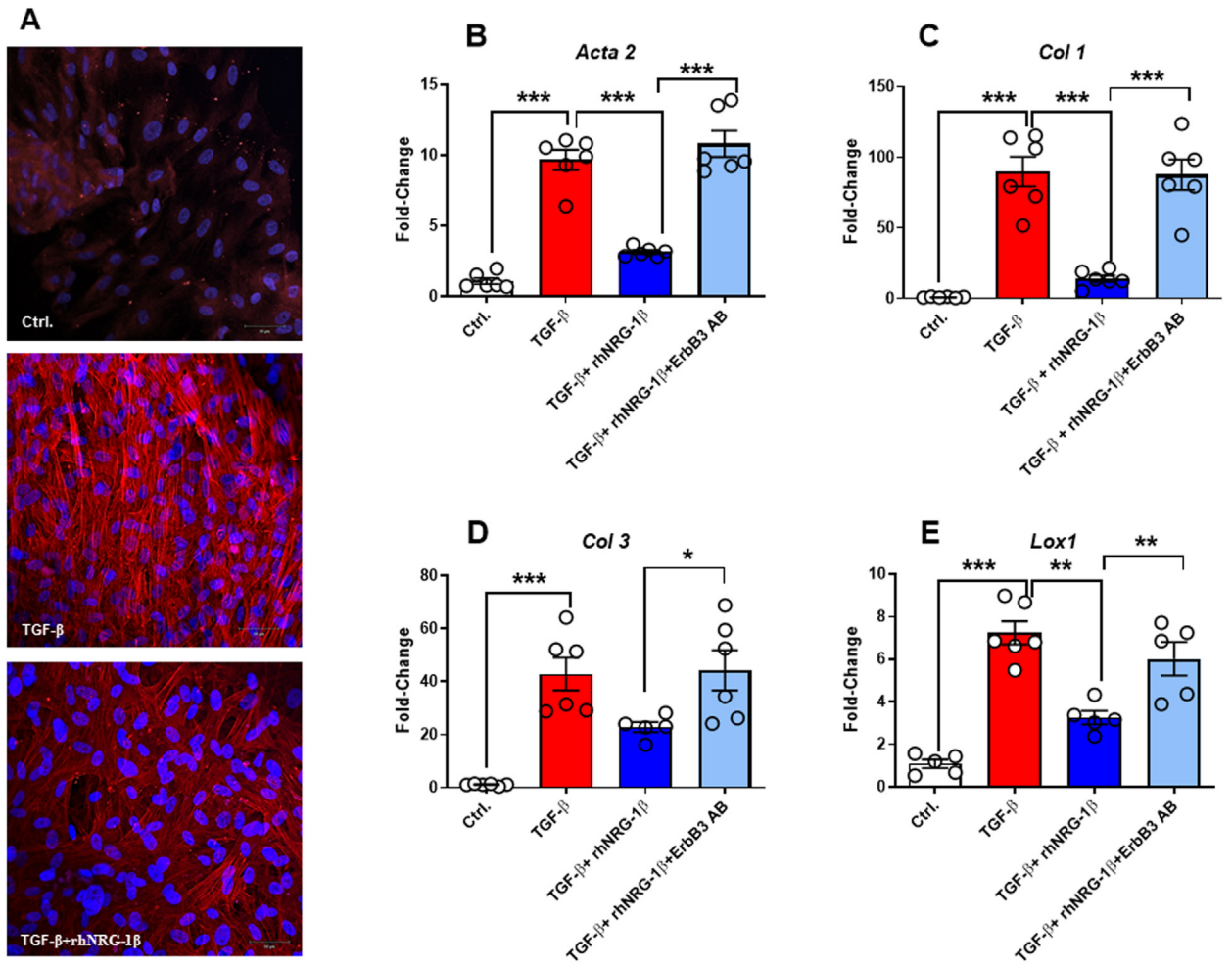


**(A)** Representative 4,6-diamidino-2-phenylindole (DAPI) and αSMA staining of human ventricular cardiac fibroblasts. The mRNA expression of **(B)** *α SMA*, alpha-smooth muscle actin; **(C)** *Col 1*, collagen 1; **(D)** *Col 3*, collagen 3; and *LOX1*, lysyl oxidase 1 in human ventricular cardiac fibroblasts. Scale bar, 50 μm. Data are expressed as mean ± SEM, n = 6 replicates/group; $*P < 0.05$, $**P < 0.01$, $***P < 0.01$, one-way analysis of variance, Tukey post hoc test. Ctrl = control; TGF-β = transforming growth factor beta; ErbB3 AB = EbB3 antibody; other abbreviations as in Figure 1.

the kidney did not show a difference among the groups (Supplemental Figures 5A and 5C). In the cardiac tissue, the *ErbB2* expressions showed no significant differences between the groups (Supplemental Figure 5D). Interestingly, the cardiac *ErbB3* and *ErbB4* transcript levels were significantly increased in response to rhNRG-1β compared with the untreated CKD group (Supplemental Figures 5E and 5F).

To demonstrate the role of ErbB3 in the NRG-1β-mediated antifibrotic process, we applied siRNA-ErbB3 and ErbB3-specific antibody (Supplemental Table 6). The silencing of ErbB3 or application of antibody against ErbB3 significantly abrogated the antifibrotic effects of rhNRG-1β (Supplemental Figure 6, **Figures 5B to 5E**).

Isolated murine primary CMs were exposed to Ang II to assess the CM-specific effects. Accordingly, the cells showed a substantial increase in markers of stretch (A-type natriuretic peptide and *Nppb*), inflammation (tumor necrosis factor-alpha), and nitro-oxidative stress (NADPH oxidase isoforms 2 and 4 [*Nox2* and *Nox4*], and 3-nitrotyrosine) (**Figures 6A to 6F**). In contrast, rhNRG-1β treatment significantly blunted these mRNA expressional changes, and there was no significant difference in the 3-nitrotyrosine

**FIGURE 6** The Effect of rhNRG-1β on the Isolated Murine Cardiomyocytes Treated by ANG II

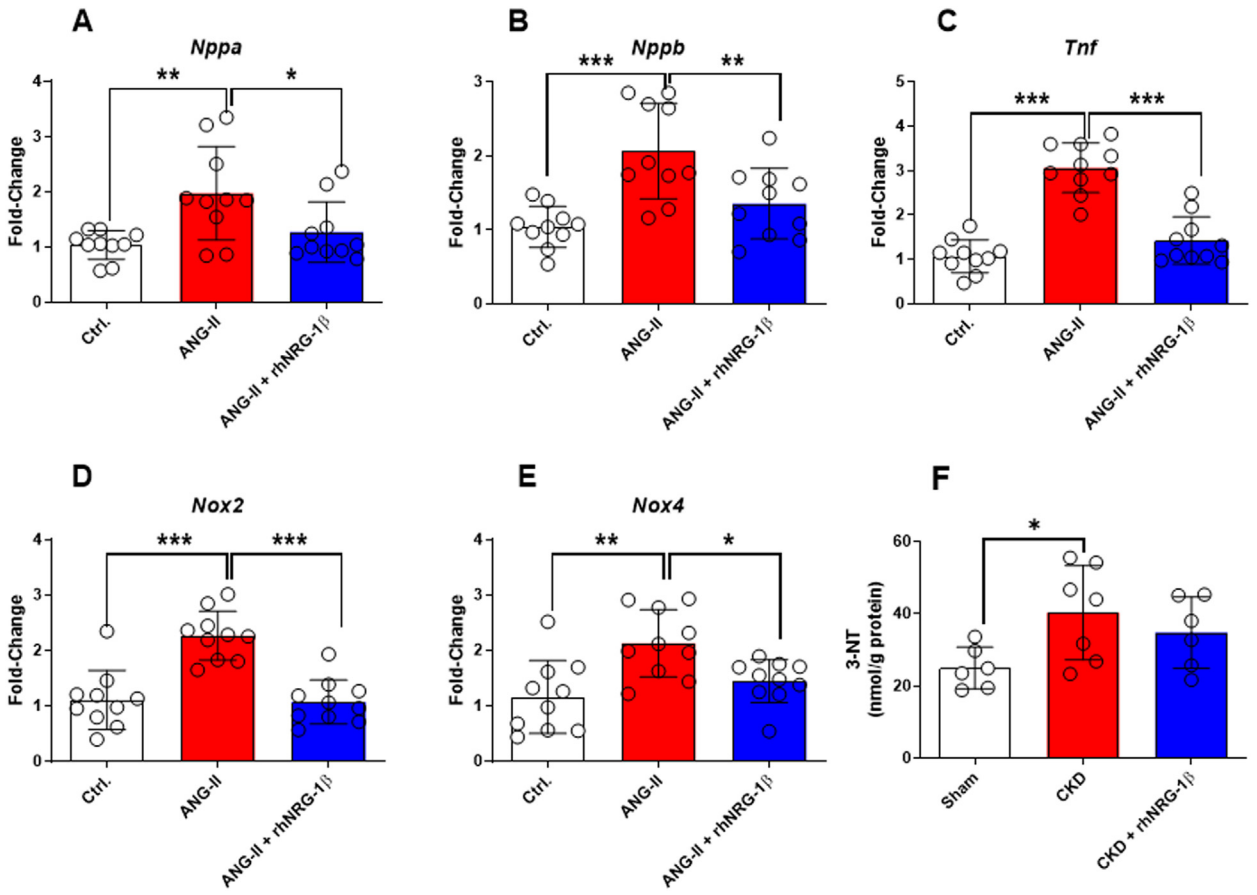


**(A)** *Nppa*, A-type natriuretic peptide, **(B)** *Nppb*, B-type natriuretic peptide, **(C)** *Tnf*, tumor necrosis factor-alpha, **(D)** *Nox2*, NADPH oxidase isoform 2, **(E)** *Nox4*, NADPH oxidase isoform 4, and **(F)** 3-NT, 3-nitrotyrosine. Data are expressed as mean ± SEM, n = 10 replicates/group; *$P < 0.05$, **$P < 0.01$ and ***$P < 0.01$, one-way analysis of variance, Tukey post hoc test. ANG II + angiotensin II. Abbreviations as in Figure 1.

levels between the sham-operated and rhNRG-1β-treated CKD groups (Figures 6A to 6F).

## DISCUSSION

The present study demonstrates, to our knowledge, for the first time that rhNRG-1β treatment prevents the progression of renal dysfunction and uremic cardiomyopathy and decreases the circulating uremic toxin levels in a rat model of CKD. The rhNRG-1β was administered in an early phase of CKD development, that is, 2 weeks after CKD induction, to investigate its therapeutic potential. In addition, this protocol reflects the clinical application of rhNRG-1β in patients with HF.[20] The rhNRG-1β treatment significantly alleviated diastolic dysfunction, fibrosis, inflammation, and oxidative stress markers in the LVs of CKD animals. In addition, the direct cardioprotective effects of rhNRG-1β were further confirmed in HVCFs and mouse CMs in vitro. Moreover, rhNRG-1β treatment decreased plasma uremic toxins levels and renal fibrosis, further supporting its indirect effects on uremic cardiomyopathy.

Our study identified that NRG-1β protein levels markedly decreased in LV and kidney tissues in CKD animals compared with the sham-operated group. A recent high-throughput proteomics study demonstrated that normalized serum NRG-1β levels were associated strongly with recovered kidney function in patients with acute kidney injury and dialysis.[31]

Inversely, the downregulation of NRG-1β-mediated signaling in the kidney may play a role in the progression of renal dysfunction.

In consonance with previous results, animals with CKD showed progressive LVH and deterioration of diastolic function,[18,19,21,32,33] albeit those symptoms were not detectable up to 4 weeks after 5/6 nephrectomy. However, characteristic laboratory changes of CKD, including elevated serum urea and creatinine concentrations, urine protein levels, and a decrease in creatinine clearance, were evidenced at week 4 in the 5/6 nephrectomy CKD model. These findings suggest that renal dysfunction has developed already during the early phase of CKD. In most cases, routine laboratory screening tests reveal the signs of CKD at this stage in patients. Therefore, we aimed to start rhNRG-1β treatment in a relatively early and asymptomatic phase of CKD in the absence of uremic cardiomyopathy (ie, before the development of LVH, diastolic dysfunction, and concomitant fibrosis), mimicking the clinical scenario. To investigate its therapeutic potential, rhNRG-1β was applied for 10 consecutive days, then the treatment was terminated, and the final results were evaluated 10 weeks after CKD initialization. This protocol has been addressed by Gao et al[20] in a phase II, randomized, double-blind, multicenter, placebo-controlled study. Patients were randomly assigned to 4 groups, treated with placebo or rhNRG-1β (0.3, 0.6, or 1.2 μg/kg/d) for 10 consecutive days and followed for 90 days.[20] It is important to emphasize that even at day 90, that is, 80 days after treatment, the LV ejection fraction remained at a high level compared with baseline or placebo treatment group values.[20] Encouraged by these important findings, we designed a similar study protocol to test the efficacy of rhNRG-1β in our CKD model.

Based on our present laboratory tests and echocardiographic findings, the severity of CKD in our model corresponds with human G2 or G3a stages, with mildly or moderately decreased kidney function at week 10.[34,35] Renal function worsened between weeks 4 and 10 in the untreated CKD group. In contrast, serum creatinine and urine protein did not show substantial changes between 4 and 10 weeks in the rhNRG-1β-treated group, highlighting its renoprotective effects. Moreover, the rhNRG-1β treatment significantly reduced the prohypertrophic and profibrotic circulatory uremic toxin levels in CKD, suggesting indirect effects on uremic cardiomyopathy. Consonantly, previous studies also demonstrated the protective effects of NRG-1β in a mouse model of type 1 diabetes mellitus and Ang II–induced cardiorenal dysfunction, respectively.[36,37]

Severe hypertension is usually not a typical feature of CKD in the 5/6 nephrectomy-induced model.[33] Consonantly, our CKD model showed a significant increase in systolic arterial blood pressure and moderately elevated diastolic and mean arterial blood pressure. We observed significantly less LVH and fibrosis in the rhNRG-1β-treated group compared with the untreated CKD group by a similar degree of systolic blood pressure elevation. Therefore, we suggest that the factors involved in the development of diastolic dysfunction and fibrosis may not be linked primarily with arterial hypertension in this animal model of CKD.

Both preclinical and clinical studies showed that uremic toxins, the overactivation of the renin-angiotensin-aldosterone system and sympathetic nervous system, increased nitro-oxidative stress, and inflammation contribute to the development of uremic cardiomyopathy.[7,38] Indeed, the observed elevation of plasma uremic toxin levels, LVH, diastolic dysfunction, and cardiac fibrosis 10 weeks after 5/6 nephrectomy were associated with significant overexpression of *Ace1*, *Agtr1*, and *Il6* in the LV tissue. Additionally, tendentiously increased renal ACE1 activity was observed in the CKD group compared with the sham-operated group, which was slightly decreased after rhNRG-1β treatment. In line with our findings, Eräranta et al[39] also found an increase in kidney ACE expression in the surgical 5/6 nephrectomy rat model. More recently, we have demonstrated that the Ang II receptor blocker losartan (10 mg/kg/d by mouth from week 5 to week 13) significantly decreased the urine volume, LVH, fibrosis, and improved diastolic dysfunction in association with a marked decrease of the LV expressions of fibrotic and inflammatory markers in an identical CKD model.[19] Therefore, we may speculate that the combination of renin-angiotensin-aldosterone system inhibitors and rhNRG-1β treatment would have a synergic cardiorenal benefit, but further studies are warranted to clarify that. The role of Ang II in LVH has also been supported by the study of Okabe et al,[40] showing a marked decreased of LVH after the suppression of the NOX4 signaling. Our data demonstrated that rhNRG-1β effectively prevented Ang II–induced CM hypertrophy, inflammation, and LV nitro-oxidative stress in concordance with previous findings.[40] Although several studies already demonstrated the anti-remodeling effects of NRG-1β in different models of heart disease, we showed for the

first time that rhNRG-1β markedly alleviates the overexpression of *Nox2* and *Nox4* in isolated murine CMs exposed to Ang II. Similar to our present findings, the increase in *Nox2* and *Nox4* expression was associated with CM dysfunctions.[41,42]

Cardiac fibrosis is central to the pathology of HF and uremic cardiomyopathy.[43] Ample HF treatment modalities target fibrotic pathways indirectly, but a specific and clinically effective antifibrotic therapy remains elusive. Therefore, new approaches are needed urgently. In the present study, the application of rhNRG-1β for 10 days resulted in a massive decrease in the progression of LV fibrosis, expression of extracellular matrix remodeling genes, and macrophage infiltration. These results are consistent with previous findings to show the antifibrotic effects of NRG-1β via the ErbB4 receptor in macrophages.[15] In addition, previous studies demonstrated the impact of NRG-1β on macrophages in different models of CVD.[15,44,45] Recent pioneering studies have confirmed the causative role of tissue macrophages in the development of diastolic dysfunction.[46,47] In our present study, at week 10, we found that rhNRG-1β-treated rats showed significantly less CD68-positive macrophage infiltration in LV tissue, which may contribute at least partially to the improvement in diastolic dysfunction.

Moreover, Yin et al[48] demonstrated that ErbB3 signaling in myeloid cells could be extrapolated to responses in cardiac pressure overload. Based on the Human Protein Atlas, the expression of ErbB3 is comparable between immune cells and cardiac fibroblasts.[49] Therefore, we investigated the effects of rhNRG-1β on the transition from cardiac fibroblast to myofibroblast via the ErbB3 receptor. We found that siRNA-ErbB3 (Supplemental Figure 6) or ErbB3 antibody administration eliminated the protective effect of rhNRG-1β in cardiac fibroblasts inferred from the *Col1* and *Col3* expressions. In addition, rhNRG-1β ameliorated the *ErbB3* repression in the LV samples and increased the *ErbB3* and *ErbB4* expressions in our CKD model. These findings suggest the causative role of ErbB3- and ErbB4-mediated signal transduction in cardiac and/or renal fibrosis and the antifibrotic effects of NRG-1β.

**STUDY LIMITATIONS.** We intended to test the therapeutic effects of rhNRG-1β in a rat model of uremic cardiomyopathy, which represents a limitation of our study. Significant differences exist in the pathomechanisms of experimental and clinical CKD, comprising the used juvenile inbred rat species, the absence of atherosclerosis and diabetes mellitus, less pronounced hypertension, and earlier development of HF. Notably, female sex could slow down the progression and severity of CKD and uremic cardiomyopathy owing to female sex hormonal effects.[1,21,50] Therefore, only male rats were used in the present study. Animal models of both sexes with concomitant comorbidities and advanced aging would be more suitable to mirror the clinical scenario of CKD in future studies. In addition, we only measured the mRNA levels of ErbB2-4 in both kidney and tissue samples; further studies are warranted to clarify and measure the protein or phospho-protein expressions of ErbB2-4 at different stages of CKD. Moreover, there remain many unknown mechanisms in the development of CKD and uremic cardiomyopathy.

## CONCLUSIONS

The rhNRG-1β treatment improved uremic cardiomyopathy and prevented the progression of renal dysfunction in association with a marked decline of circulating uremic toxins in a rat model of CKD. Therefore, rhNRG-1β may represent a novel promising therapeutic strategy in translational studies aiming to treat CKD-induced cardiomyopathy in type 4 cardiorenal syndrome. RhNRG-1 has already been tested in accomplished clinical trials targeting chronic HF, and at least 3 studies are recruiting patients for ongoing studies (https://clinicaltrials.gov). Gao et al[20] reported a moderate but nonsignificant increase of LV ejection fraction vs placebo in a phase II, randomized, double-blind, multicenter, placebo-controlled trial. Jabbour et al[51] used an intravenous infusion of rhNRG-1β2a isoform for 11 days in their phase I trial with a favorable improvement of hemodynamic function, but with adverse side effects detected already in a very small group of patients. To avoid further negative clinical trials, we warrant multiple dose-finding and mechanistic studies in different preclinical models, including large animals, which better mimic the clinical setting. Considering the broad expression of ErbB3 receptor,[52] the investigation of side effects should include multiple organs and should include animal models demonstrating a combination of HF with reduced ejection fraction with typical comorbidities. The activation of ErbB receptors is implicated in tumor development; consequently, a standard oncologic screening will be highly recommended during the design of clinical trials.[52] We would like to emphasize the novel, proof-of-concept character of our study in uremic cardiomyopathy, in which a single dose of rhNRG-1β administered for 10 days improved the cardiac and

kidney function and paved the route for drug development strategies.

## FUNDING SUPPORT AND AUTHOR DISCLOSURES

The present work was supported by the Ludwig Boltzmann Institute for Cardiovascular Research, Vienna, Austria, and the projects of Österreichischer Austauschdienst (OMAA Projekt 100öu3), and the National Research, Development and Innovation Office, Hungary (GINOP-2.3.2-15-2016-00040, NKFIH FK129094, and EFOP-3.6.2-16-2017-00006). Dr Kiss was supported by Theodor Körner Founds. Drs Sárközy and Kovács were supported by the New National Excellence Program of the Ministry of Human Capacities, Hungary (UNKP-20-5-SZTE-166 and UNKP-19-3-SZTE-160). Dr Sárközy was supported by the János Bolyai Research Fellowship of the Hungarian Academy of Sciences. Dr Kovács was supported by the EFOP 3.6.3-VEKOP-16-2017-00009 (Hungary). Dr Márványkövi was supported by the Szeged Scientists Academy Program (TSZ:34232-3/2016/INTFIN, Hungary). Single-Cell Technologies Ltd., Szeged, Hungary, developed the Biology Image Analysis Software (BIAS). Dr Horváth is the CEO and Mr Kovács is a software engineer at Single-Cell Technologies Ltd. All other authors have reported that they have no relationships relevant to the contents of this paper to disclose.

**ADDRESS FOR CORRESPONDENCE:** Dr Attila Kiss, Ludwig Boltzmann Institute for Cardiovascular Research at Center for Biomedical Research and Translational Surgery, Medical University of Vienna, Vienna, Währinger Gürtel 18-20, A-1090, Austria. E-mail: attila.kiss@meduniwien.ac.at.

## PERSPECTIVES

**COMPETENCY IN MEDICAL KNOWLEDGE:** CKD is a global health problem affecting 10% to 12% of the population. Uremic cardiomyopathy is defined by CKD-associated chronic and often irreversible structural and functional changes of the heart. It comprises LVH, diastolic dysfunction, and cardiac fibrosis, ultimately leading to HF (ie, type 4 cardiorenal syndrome). Inflammation and dysregulation of endothelium-derived NRG-1β signaling are known contributors to HF with different etiologies. Here, we showed that the daily systemic administration of rhNRG-1β for 10 days in our rat model of CKD induced by 5/6 nephrectomy alleviated the progression of uremic cardiomyopathy and kidney dysfunction.

**TRANSLATIONAL OUTLOOK:** Our present study identified rhNRG-1β as a novel promising druggable candidate in the prevention and therapy of uremic cardiomyopathy and renal dysfunction in type 4 cardiorenal syndrome. The currently presented positive preclinical data warrant clinical studies to confirm the beneficial effects of rhNRG-1β in patients with CKD.

## REFERENCES

**1.** GBD Chronic Kidney Disease Collaboration. Global, regional, and national burden of chronic kidney disease, 1990-2017: a systematic analysis for the Global Burden of Disease Study 2017. *Lancet*. 2020;395(10225):709-733.

**2.** Romagnani P, Remuzzi G, Glassock R, et al. Chronic kidney disease. *Nat Rev Dis Primers*. 2017;3:17088.

**3.** Duni A, Liakopoulos V, Rapsomanikis K-P, Dounousi E. Chronic kidney disease and disproportionally increased cardiovascular damage: does oxidative stress explain the burden? *Oxid Med Cell Longev*. 2017;2017:9036450.

**4.** Saran R, Robinson B, Abbott KC, et al. US Renal Data System 2018 annual data report: epidemiology of kidney disease in the United States. *Am J Kidney Dis*. 2019;73(3 Suppl 1):A7-A8.

**5.** Ronco C, Haapio M, House AA, Anavekar N, Bellomo R. Cardiorenal syndrome. *J Am Coll Cardiol*. 2008;52(19):1527-1539.

**6.** Husain-Syed F, McCullough PA, Birk H-W, et al. Cardio-pulmonary-renal interactions: a multidisciplinary approach. *J Am Coll Cardiol*. 2015;65(22):2433-2448.

**7.** Sárközy M, Kovács ZZA, Kovács MG, Gáspár R, Szűcs G, Dux L. Mechanisms and modulation of oxidative/nitrative stress in type 4 cardio-renal syndrome and renal sarcopenia. *Front Physiol*. 2018;9:1648.

**8.** Wang X, Shapiro JI. Evolving concepts in the pathogenesis of uraemic cardiomyopathy. *Nat Rev Nephrol*. 2019;15(3):159-175.

**9.** Falconi CA, Da Junho CVC, Fogaça-Ruiz F, et al. Uremic toxins: an alarming danger concerning the cardiovascular system. *Front Physiol*. 2021;12:686249.

**10.** Lekawanvijit S, Kompa AR, Krum H. Protein-bound uremic toxins: a long overlooked culprit in cardiorenal syndrome. *Am J Physiol Renal Physiol*. 2016;311(1):F52-F62.

**11.** Hedhli N, Huang Q, Kalinowski A, et al. Endothelium-derived neuregulin protects the heart against ischemic injury. *Circulation*. 2011;123(20):2254-2262.

**12.** Geissler A, Ryzhov S, Sawyer DB. Neuregulins: protective and reparative growth factors in multiple forms of cardiovascular disease. *Clin Sci (Lond)*. 2020;134(19):2623-2643.

**13.** Liu X, Gu X, Li Z, et al. Neuregulin-1/erbB-activation improves cardiac function and survival in models of ischemic, dilated, and viral cardiomyopathy. *J Am Coll Cardiol*. 2006;48(7):1438-1447.

**14.** Hopf A-E, Andresen C, Kötter S, et al. Diabetes-induced cardiomyocyte passive stiffening is caused by impaired insulin-dependent titin modification and can be modulated by neuregulin-1. *Circ Res*. 2018;123(3):342-355.

**15.** Vermeulen Z, Hervent A-S, Dugaucquier L, et al. Inhibitory actions of the NRG-1/ErbB4 pathway in macrophages during tissue fibrosis in the heart, skin, and lung. *Am J Physiol Heart Circ Physiol*. 2017;313(5):H934-H945.

**16.** Wang B, Wang Z-M, Ji J-L, et al. Macrophage-derived exosomal Mir-155 regulating cardiomyocyte pyroptosis and hypertrophy in uremic cardiomyopathy. *J Am Coll Cardiol Basic Trans Sci*. 2020;5(2):148-166.

**17.** Winterberg PD, Robertson JM, Kelleman MS, George RP, Ford ML. T cells play a causal role in diastolic dysfunction during uremic cardiomyopathy. *J Am Soc Nephrol*. 2019.

**18.** Sárközy M, Gáspár R, Zvara Á, et al. Chronic kidney disease induces left ventricular overexpression of the pro-hypertrophic microRNA-212. *Sci Rep*. 2019;9(1):1302.

**19.** Kovács ZZA, Szűcs G, Freiwan M, et al. Comparison of the antiremodeling effects of losartan and mirabegron in a rat model of uremic cardiomyopathy. *Sci Rep*. 2021;11(1):17495.

**20.** Gao R, Zhang J, Cheng L, et al. A Phase II, randomized, double-blind, multicenter, based on standard therapy, placebo-controlled study of the efficacy and safety of recombinant human neuregulin-1 in patients with chronic heart failure. *J Am Coll Cardiol*. 2010;55(18):1907-1914.

**21.** Sárközy M, Márványkövi FM, Szűcs G, et al. Ischemic preconditioning protects the heart

against ischemia-reperfusion injury in chronic kidney disease in both males and females. *Biol Sex Differ*. 2021;12(1):49.

**22.** Kocsis GF, Sárközy M, Bencsik P, et al. Preconditioning protects the heart in a prolonged uremic condition. *Am J Physiol Heart Circ Physiol*. 2012;303(10):H1229–H1236.

**23.** Pilz PM, Hamza O, Gidlöf O, et al. Remote ischemic preconditioning attenuates adverse cardiac remodeling and preserves left ventricular function in a rat model of reperfused myocardial infarction. *Int J Cardiol*. 2019;285:72–79.

**24.** Hamza O, Kiss A, Kramer A-M, et al. Tenascin C promotes valvular remodeling in two large animal models of ischemic mitral regurgitation. *Basic Res Cardiol*. 2020;115(6):76.

**25.** Ackers-Johnson M, Li PY, Holmes AP, O'Brien S-M, Pavlovic D, Foo RS. A Simplified, Langendorff-free method for concomitant isolation of viable cardiac myocytes and nonmyocytes from the adult mouse heart. *Circ Res*. 2016;119(8):909–920.

**26.** Galla Z, Rajda C, Rácz G, et al. Simultaneous determination of 30 neurologically and metabolically important molecules: a sensitive and selective way to measure tyrosine and tryptophan pathway metabolites and other biomarkers in human serum and cerebrospinal fluid. *J Chromatogr A*. 2021;1635:461775.

**27.** Galla Z, Rácz G, Grecsó N, et al. Improved LC-MS/MS method for the determination of 42 neurologically and metabolically important molecules in urine. *J Chromatogr B Analyt Technol Biomed Life Sci*. 2021;1179:122846.

**28.** Kovács MG, Kovács ZZA, Varga Z, et al. Investigation of the Antihypertrophic and antifibrotic effects of losartan in a rat model of radiation-induced heart disease. *Int J Mol Sci*. 2021;22(23).

**29.** Freiwan M, Kovács MG, Kovács ZZA, et al. Investigation of the antiremodeling effects of losartan, mirabegron and their combination on the development of doxorubicin-induced chronic cardiotoxicity in a rat model. *Int J Mol Sci*. 2022;23(4).

**30.** Szabó PL, Ebner J, Koenig X, et al. Cardiovascular phenotype of the Dmdmdx rat - a suitable animal model for Duchenne muscular dystrophy. *Dis Model Mech*. 2021;14(2).

**31.** Daniels JR, Ma JZ, Cao Z, et al. Discovery of novel proteomic biomarkers for the prediction of kidney recovery from dialysis-dependent AKI patients. *Kidney360*. 2021;2(11):1716–1727.

**32.** Švíglerová J, Kuncová J, Nalos L, Tonar Z, Rajdl D, Stengl M. Cardiovascular parameters in rat model of chronic renal failure induced by subtotal nephrectomy. *Physiol Res*. 2010;59(Suppl 1):S81–S88.

**33.** Hewitson TD, Holt SG, Smith ER. Animal models to study links between cardiovascular disease and renal failure and their relevance to human pathology. *Front Immunol*. 2015;6:465.

**34.** Clementi A, Virzì GM, Goh CY, et al. Cardiorenal syndrome type 4: a review. *Cardiorenal Med*. 2013;3(1):63–70.

**35.** Da Pinheiro Silva AL, Da Vaz Silva MJ. Type 4 cardiorenal syndrome. *Rev Port Cardiol*. 2016;35(11):601–616.

**36.** Vandekerckhove L, Vermeulen Z, Liu ZZ, et al. Neuregulin-1 attenuates development of nephropathy in a type 1 diabetes mouse model with high cardiovascular risk. *Am J Physiol Endocrinol Metab*. 2016;310(7):E495–E504.

**37.** Shakeri H, Boen JRA, Moudt S de, et al. Neuregulin-1 compensates for endothelial nitric oxide synthase deficiency. *Am J Physiol Heart Circ Physiol*. 2021;320(6):H2416–H2428.

**38.** Kaesler N, Babler A, Floege J, Kramann R. Cardiac remodeling in chronic kidney disease. *Toxins (Basel)*. 2020;12(3):161.

**39.** Eräranta A, Riutta A, Fan M, et al. Dietary phosphate binding and loading alter kidney angiotensin-converting enzyme mRNA and protein content in 5/6 nephrectomized rats. *Am J Nephrol*. 2012;35(5):401–408.

**40.** Okabe K, Matsushima S, Ikeda S, et al. DPP (dipeptidyl peptidase)-4 inhibitor attenuates Ang II (angiotensin II)-induced cardiac hypertrophy via GLP (glucagon-like peptide)-1-dependent suppression of Nox (nicotinamide adenine dinucleotide phosphate oxidase) 4-HDAC (histone deacetylase) 4 pathway. *Hypertension*. 2020;75(4):991–1001.

**41.** Heymes C, Bendall JK, Ratajczak P, et al. Increased myocardial NADPH oxidase activity in human heart failure. *J Am Coll Cardiol*. 2003;41(12):2164–2171.

**42.** Looi YH, Grieve DJ, Siva A, et al. Involvement of Nox2 NADPH oxidase in adverse cardiac remodeling after myocardial infarction. *Hypertension*. 2008;51(2):319–325.

**43.** Sweeney M, Corden B, Cook SA. Targeting cardiac fibrosis in heart failure with preserved ejection fraction: mirage or miracle? *EMBO Mol Med*. 2020;12(10):e10865.

**44.** Shiraishi M, Yamaguchi A, Suzuki K. Nrg1/ErbB signaling-mediated regulation of fibrosis after myocardial infarction. *FASEB J*. 2022;36(2):e22150.

**45.** Pascual-Gil S, Abizanda G, Iglesias E, Garbayo E, Prósper F, Blanco-Prieto MJ. NRG1 PLGA MP locally induce macrophage polarisation toward a regenerative phenotype in the heart after acute myocardial infarction. *J Drug Target*. 2019;27(5-6):573–581.

**46.** Hulsmans M, Sager HB, Roh JD, et al. Cardiac macrophages promote diastolic dysfunction. *J Exp Med*. 2018;215(2):423–440.

**47.** Mouton AJ, Li X, Hall ME, Hall JE. Obesity, hypertension, and cardiac dysfunction: novel roles of immunometabolism in macrophage activation and inflammation. *Circ Res*. 2020;126(6):789–806.

**48.** Yin H, Favreau-Lessard AJ, deKay JT, et al. Protective role of ErbB3 signaling in myeloid cells during adaptation to cardiac pressure overload. *J Mol Cell Cardiol*. 2021;152:1–16.

**49.** The Human Protein Atlas. ENSG00000065361-ERBB3/tissue. Accessed March 10, 2023. Available at: https://www.proteinatlas.org/search/ENSG00000065361-ERBB3%2Ftissue

**50.** Carrero JJ, Hecking M, Chesnaye NC, Jager KJ. Sex and gender disparities in the epidemiology and outcomes of chronic kidney disease. *Nat Rev Nephrol*. 2018;14(3):151–164.

**51.** Jabbour A, Hayward CS, Keogh AM, et al. Parenteral administration of recombinant human neuregulin-1 to patients with stable chronic heart failure produces favourable acute and chronic haemodynamic responses. *Eur J Heart Fail*. 2011;13(1):83–92.

**52.** Wang Z. ErbB Receptors and Cancer. *Methods Mol Biol*. 2017;1652:3–35.

**KEY WORDS** cardiac fibrosis, chronic kidney disease, left ventricular hypertrophy, recombinant human neuregulin-1β, uremic cardiomyopathy

**APPENDIX** For a supplemental Methods section as well as tables and figures, please see the online version of this paper.